Shielding effects of myelin sheath on axolemma depolarization under transverse electric field stimulation

Hui Ye and Jeffrey Ng

Department of Biology, Loyola University of Chicago, Chicago, IL, USA

ABSTRACT

Axonal stimulation with electric currents is an effective method for controlling neural activity. An electric field parallel to the axon is widely accepted as the predominant component in the activation of an axon. However, recent studies indicate that the transverse component to the axolemma is also effective in depolarizing the axon. To quantitatively investigate the amount of axolemma polarization induced by a transverse electric field, we computed the transmembrane potential (*Vm*) for a conductive body that represents an unmyelinated axon (or the bare axon between the myelin sheath in a myelinated axon). We also computed the transmembrane potential of the sheath-covered axonal segment in a myelinated axon. We then systematically analyzed the biophysical factors that affect axonal polarization under transverse electric stimulation for both the bare and sheath-covered axons. Geometrical patterns of polarization of both axon types were dependent on field properties (magnitude and field orientation to the axon). Polarization of both axons was also dependent on their axolemma radii and electrical conductivities. The myelin provided a significant "shielding effect" against the transverse electric fields, preventing excessive axolemma depolarization. Demyelination could allow for prominent axolemma depolarization in the transverse electric field, via a significant increase in myelin conductivity. This shifts the voltage drop of the myelin sheath to the axolemma. Pathological changes at a cellular level should be considered when electric fields are used for the treatment of demyelination diseases. The calculated term for membrane polarization (*Vm*) could be used to modify the current cable equation that describes axon excitation by an external electric field to account for the activating effects of both parallel and transverse fields surrounding the target axon.

Subjects Biophysics, Computational Biology, Mathematical Biology, Neurology
Keywords Transverse field, Axon, Shielding effect, Myelin, Cable equation, Electric stimulation

INTRODUCTION

Electrical stimulation of nerve cells was first reported by Luigi Galvani in 1780 (*Galvani, 1791*), who accidently found that muscles from a dead frog would twitch when touched with a charged metal scalpel, a discovery that sparked the appreciation of electricity in relation to animation—or life. Today, electric stimulation of neurons in the peripheral or central nervous systems have been widely utilized for controlling neural

Submitted 15 May 2018
Accepted 29 October 2018
Published 3 December 2018

Corresponding author
Hui Ye, hye1@luc.edu

Academic editor
Tjeerd Boonstra

Additional Information and Declarations can be found on page 16

DOI **10.7717/peerj.6020**

network activity (*Selimbeyoglu & Parvizi, 2010*), synaptic transmission (*Nowak & Bullier, 1998*), and pain (*Coderre et al., 1993*). Electric currents can also be generated via magneto-electric induction with magnetic coils for non-invasive control of neural activity (*Maccabee et al., 1991*, *1993*; *Ye et al., 2010*, *2011*; *Ye & Steiger, 2015*).

An electric field surrounding a straight nerve axon can be separated into two components: one parallel to ($E_{//}$) and the other perpendicular (traversal, $E_{\perp}$) to the axon. The $E_{//}$ is widely regarded as the predominant factor that activates the axons (*Basser, Wijesinghe & Roth, 1992*; *Roth & Basser, 1990*), which is supported by numerous experimental results (*Amassian, Maccabee & Cracco, 1989*; *Basser & Roth, 2000*). Consequently, theoretical analyses of electrical activation have predominately been focused on computing $E_{//}$ along a fiber (*Esselle & Stuchly, 1994*, *1995*; *Nagarajan & Durand, 1995*; *Ravazzani et al., 1996*; *Roth & Basser, 1990*; *Roth et al., 1990*). The current cable equation, $\lambda^2 \frac{\partial^2 \phi_m}{\partial x^2} - \tau \frac{\partial \phi_m}{\partial t} - \phi_m = -\lambda^2 \frac{\partial V_e}{\partial x^2}$, which describes axonal activation, contains only the axial term ($E_{//}$). Here, $\lambda^2 = \frac{R_m c}{2R_i}$ and $\tau = R_m C_m$ are the space and time constants, respectively. ϕ_m is the transmembrane potential and V_e is the extracellular electric field applied to the fiber. It is nonzero only if $E_{//}$ is nonzero. The surface resistance and capacitance of the membrane are R_m and C_m, respectively. The intracellular resistivity is R_i and the fiber radius is c. This simplification facilities the rapid calculation of neural activation. However, it ignores the presence of the cell, which perturbs the local extracellular electric field. It also ignores the mutual interactions between the neurons and the applied electric field (*Ye & Steiger, 2015*), mainly the electric field that directly penetrates and depolarizes the cell membrane, or $E_{\perp}$.

Transversal field for membrane polarization

Mounting evidence from experimental and simulation studies support the notion that cell membranes can be polarized by transversal electric fields. An electric field that penetrates the cell membrane was directly observed to cause polarization in hippocampal neurons (*Bikson et al., 2001*), in neural stem cells (*Zhao et al., 2015*), and in oocytes (*Lee & Grill, 2005*). When $E_{\perp}$ is extremely strong, it can even cause membrane instability and pore formation (*Bingham, Olmsted & Smye, 2010*). Analytical computations of the transverse membrane potential under electric stimulation started as early as the 1950s (*Fricke, 1953*; *Schwan, 1957*) for a simple cellular shape. Recent works have calculated membrane polarization by the transverse field in cells with more complex geometry (*Kotnik & Miklavcic, 2000a*, *2000b*), and by the transverse electric field induced by time-varying magnetic field (*Ye, Cotic & Carlen, 2007*; *Ye et al., 2011*).

Because of the observable, polarizing effects of the transverse field on large structures like the cell body, it is reasonable to speculate that a transverse field could also play a significant role in the polarization of axons. Indeed, evidence favoring transversal activation of axons also appear in the literature. It was reported (*Pourtaheri et al., 2009*) that individual axons can be selectively activated by a transverse field in a nerve bundle. These fields produce strong effects in the stimulation of ulnar nerves (*Cros, Day & Shahani, 1990*; *Olney et al., 1990*) and long fibers (*Grill & Wei, 2009*). Using a magnetic

coil to induce the electric field, *Ruohonen et al. (1996)* discovered that activation of peripheral nerves could occur when the coil was oriented in a way that only generated $E_{\perp}$, and a later theoretical work (*Ye et al., 2011*) confirmed the axonal depolarization by this field. Clinically, the fast switching of magnetic fields during magnetic resonance imaging (MRI) scanning generates $E_{\perp}$ in patients, which is considered an important risk factor for unwanted peripheral nerve stimulation (*While & Forbes, 2004*).

At present, the consensus is that $E_{\perp}$ is a modulator to the dominant effects caused by $E_{//}$, although some researchers have speculated that the stimulation effects from transverse fields may arise due to nerve undulation, which generates longitudinal field components (*Lontis, Nielsen & Struijk, 2009*; *Schnabel & Struijk, 1999*; *Struijk & Durand, 1998*). In the presence of $E_{//}$, it was thought that $E_{\perp}$ could introduce subthreshold membrane depolarization which enhances stimulation by providing an additive effect on $E_{//}$ (*Lontis, Nielsen & Struijk, 2009*). Alternatively, $E_{\perp}$ may provide rapid axonal polarization in the transverse direction and $E_{//}$ drives the slow development of the mean transmembrane potential (*Cranford, Kim & Neu, 2012*). $E_{//}$ and $E_{\perp}$ could potentially provide a strategy for differential activation of axons with different properties (*Ruohonen et al., 1996*).

Modify cable equation to include the contribution of transverse field

In cases with significant transverse stimuli, where the membrane-field interaction is sufficient and polarization is primarily due to the transverse field, the cable model assumptions are known to be invalid (*Krassowska & Neu, 1994*). Many modeling studies have argued for the inclusion of the transverse field for the accurate simulation of neural activation, as well as the development of mathematical tools to serve this purpose (*Gimsa & Wachner, 2001*; *Kotnik & Miklavcic, 2000a*, *2006*; *Krassowska & Neu, 1994*; *Ye et al., 2011*; *Ye & Steiger, 2015*).

Several papers have reported their first endeavors for modifying the cable equation. *Yu, Zheng & Wang (2005)* modified the activation function to include the transversal field in magnetic stimulation. *Ravazzani et al. (1996)* magnetically stimulated the median nerve and recorded the evoked muscle responses, and discovered that including the transversal field in the cable equation provided a much improved correlation between the mush Electromyography (EMG) and the activating function. A recent endeavor, which modified the current cable equation to include the transversal term (*Wang et al., 2018*), showed that the transversal field could affect threshold of demyelinated axons, but not in myelinated axons. Another work by the same group included the transverse term in the cable equation that describes magnetic field stimulation (*Wang, Grill & Peterchev, 2018*). In both these studies, the membrane was represented by a resistor in parallel with a membrane capacitance. For computational simplicity, all the above-mentioned works ignored the physical presence of the lipid bilayer membrane, a "shell" like structure that has non-zero thickness. Consequently, the field perturbation caused by the membrane, which is essential for the re-distribution of the transverse field proximal to the axon (*Farkas, Korenstein & Malkin, 1984*; *Jerry, Popel & Brownell, 1996*; *Lee & Grill, 2005*; *Mossop et al., 2007*), as well as the buildup of transmembrane potential

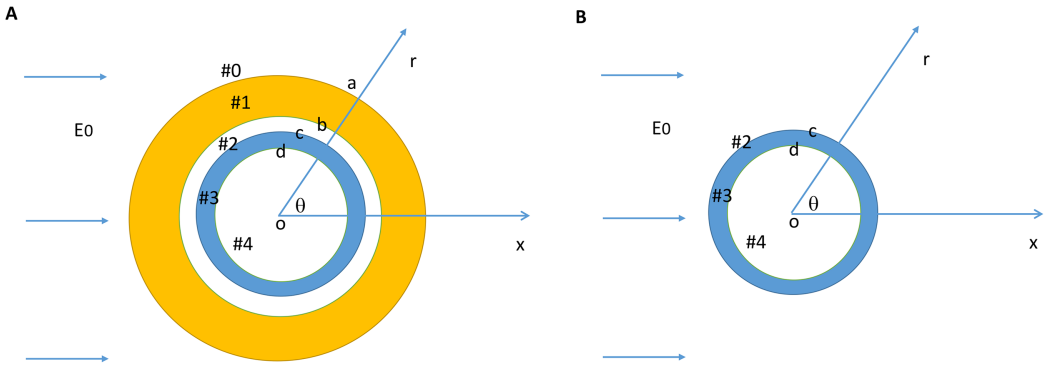

Figure 1 Model setup for a myelin-covered axon (A) and a bare axon (B) under transverse electric field stimulation. The cylindrical coordinate system that was used to define the orientation of the electric field and the axon. Full-size DOI: 10.7717/peerj.6020/fig-1

(*Kotnik & Miklavcic, 2000a*, *2000b*) through cell-field interaction (*Ye & Steiger, 2015*), were ignored. Furthermore, in the myelinated axon model, the possibility that the presence of the myelin sheath might shield the internal structure such as the axon membrane (*Kotnik & Miklavcic, 2006*; *Ye & Curcuru, 2016*) was not considered.

In the present paper, we model a bare axon as a conductive cylindrical shell, and provide an analytical expression of membrane polarization (*Vm*) for an unmyelinated axon (or the node of Ranvier in myelinated axon), under transverse electric field stimulation. We also provide *Vm* for a myelin-covered axon, which was modeled as a co-centric, two shell structure. We investigate biophysical factors that may affect the *Vm*, including field intensity and orientation, axonal biophysics and the impact of pathological demyelination. We discuss the possibility of placing *Vm* into a modified cable equation, so that the contributions of both the longitudinal and transverse components of an electrical field could be simultaneously evaluated during electric stimulation of axons.

METHODS

Cylindrical axon model in a transverse electric field

We modeled a bare axon and its myelin sheath using homogeneous cylindrical volume conductors (*Esselle & Stuchly, 1994*; *Schnabel & Struijk, 2001*). Figure 1A illustrates the location and orientation of a myelin-covered axon in a cylindrical coordinate system (r, θ, z). The axon was exposed to a transverse, direct current (DC) electric field (E_0). It included a total of five isotropic and homogenous regions: the medium (#0), the myelin sheath (#1), the periaxonal space (#2), the axolemma (#3), and the axonal cytoplasm (#4). The dielectric permittivities and conductivities in the five regions were ε_0, ε_1, ε_2, ε_3, ε_4 and σ_0, σ_1, σ_2, σ_3, σ_4, respectively. The myelin had an outer radius (a), inner radius (b), and the thickness (b–a). The axon had an outer radius (c) and inner radius (d). Thickness of the axolemma was therefore c–d. Figure 1B illustrates a bare axon, which was composed of only the periaxonal space (#2), the axolemma (#3), and the axonal cytoplasm regions.

Governing equation and boundary conditions

Using the cylindrical coordinates (r, θ, z), the electric field distribution was calculated by

$$E = -\nabla V = -\left(\frac{\partial V}{\partial r}, \frac{1}{r}\frac{\partial V}{\partial \theta}, \frac{\partial V}{\partial z}\right) \quad (1)$$

For the DC electric field stimulation, an electric potential was obtained by solving Laplace's equation

$$\nabla^2 V = 0 \quad (2)$$

The potential, V, is the electric scalar potential due to the charge accumulation between the interface of the two different media (*Stratton, 1941*). In a cylindrical coordinate system (r, θ, z), it is written as

$$\frac{1}{r}\frac{\partial}{\partial r}\left(r\frac{\partial V}{\partial r}\right) + \frac{1}{r^2}\frac{\partial^2 V}{\partial \theta^2} = 0 \quad (3)$$

Several boundary conditions were evaluated in solving the equation (Appendix): (A) The electric potential was continuous across the boundary of the two different media. (B) The normal current density was continuous across the two different media. "Complex conductivity," defined as $S = \sigma + j\omega\varepsilon$, was calculated to account for the dielectric permittivity of the material (*Kotnik & Miklavcic, 2000b*; *Kotnik, Miklavcic & Slivnik, 1998*; *Polk & Song, 1990*). Here, σ was the conductivity of the tissue, ε was the permittivity, ω was the angular frequency of the field (zero for DC electric field) and $j = \sqrt{-1}$ was the imaginary unit. On the extracellular media/myelin interface (#0#1, $r = a$),

$$S_0 E_{0r} - S_1 E_{1r} = 0 \quad (4)$$

On the myelin/periaxonal interface (#1#2, $r = b$),

$$S_1 E_{1r} - -S_2 E_{2r} = 0 \quad (5)$$

On the periaxonal/axon interface (#2#3, $r = c$),

$$S_2 E_{2r} - S_3 E_{3r} = 0 \quad (6)$$

On the axon/cytoplasm interface (#3#4, $r = d$),

$$S_3 E_{3r} - S_4 E_{4r} = 0 \quad (7)$$

where $S_0 = \sigma_0 + j\omega\varepsilon_0, S_1 = \sigma_1 + j\omega\varepsilon_1, S_2 = \sigma_2 + j\omega\varepsilon_2, S_3 = \sigma_3 + j\omega\varepsilon_3, S_4 = \sigma_4 + j\omega\varepsilon_4$. (C) Electric fields an infinite distance away should not be perturbed by presence of the axon. (D) The electric potential inside the cytoplasm ($r = 0$) was finite.

Model parameters

Table 1 lists the default values of the model parameters and their ranges. The choice of the electric parameters were based on reports in the literature (*Kotnik, Bobanovic & Miklavcic, 1997*; *Kotnik & Miklavcic, 2006*). Axon radius was selected from *Berthold & Rydmark (1995)*. The diameter of the unmyelinated axons ranges from approximately 0.1–2 μm (three μm in humans). We used 0.6 μm as the standard value and 0.1–3 μm as the range. The thickness of the axonal membrane was selected from *Nagarajan & Durand (1995)*. The diameter of the myelin was set to double the axon diameter.

Table 1 Model parameters.

Parameters	Standard value	Lower limit	Upper limit
Extracellular conductivity (σ_0, S/m)[a,b]	0.2	5×10^{-4}	2.0
Myelin conductivity (σ_1, S/m)[a,b]	5.0×10^{-7}/n[g]	1.0×10^{-8}/n	1.2×10^{-6}/n
Periaxonal conductivity (σ_2, S/m)[a,b]	0.2	2.0×10^{-2}	1.0
Axonal conductivity (σ_3, S/m)[a,b]	5.0×10^{-7}	1.0×10^{-8}	1.2×10^{-6}
Cytoplasmic conductivity (σ_4, S/m)[a,b]	0.2	2.0×10^{-2}	1.0
Extracellular dielectric permittivity (ε_0, As/*Vm*)[a,b]	6.4×10^{-10}	3.5×10^{-10}	7.0×10^{-10}
Myelin dielectric permittivity (ε_1, As/*Vm*)[a,b]	4.4×10^{-11}	1.8×10^{-11}	8.8×10^{-11}
Periaxonal dielectric permittivity (ε_2, As/*Vm*)[a,b]	6.4×10^{-10}	3.5×10^{-10}	7.0×10^{-10}
Axonal myelin dielectric permittivity (ε_3, As/*Vm*)[a,b]	4.4×10^{-11}	1.8×10^{-11}	8.8×10^{-11}
Cytoplasmic dielectric permittivity (ε_4, As/*Vm*)[a,b]	6.4×10^{-10}	3.5×10^{-10}	7.0×10^{-10}
Myelin diameter (a, *nm*)	1.5	0.7	4.6
b. Axonal membrane thickness (*nm*)[c]	6	4	8
Axonal radius (c, μm)[d]	0.6	0.1	1.2
Periaxonal space width (μm)[e]	0.004	0.004	0.004
Number of myelin layers (*n*)[f]	40	0	40
Electric field intensity (V/m)	200	0	200,000[h]

Notes:
[a] *Kotnik, Bobanovic & Miklavcic (1997)*.
[b] *Kotnik & Miklavcic (2006)*.
[c] *Nagarajan & Durand (1995)*.
[d] *Berthold & Rydmark (1995)*.
[e] *Berthold, Nilsson & Rydmark (1983)*.
[f] *Ruff et al. (2013)*.
[g] *Chomiak & Hu (2009)*.
[h] *Sadik et al. (2011)*.

Lamella are produced by many layers of processes from oligodendrocytes with significant membrane resistivity (*Bakiri et al., 2011*). The resistance of the myelin was scaled linearly by the number (*n*) of lamella (*Chomiak & Hu, 2009*). The standard electric intensity was 200 V/m. The maximum intensity is the one that can cause membrane electroporation (*Sadik et al., 2011*).

Software packages

Equations were derived with Mathematica 10 (Wolfram Research, Inc. Champaign, IL, USA). Numerical simulations were performed with Matlab 8.4.0 (The MathWorks, Inc. Natick, MA, USA).

RESULTS

Analytical expressions of axonal transmembrane potential (*Vm*) and voltage drop on the myelin sheath (ϕ) under transverse electric stimulation

The solution for Laplace's equation (Eq. (3)) was written in the form (*Griffiths, 1999*)

$$V(r,\theta) = A_0 \ln(r) + B_0 + \sum_{n=1}^{\infty} r^n [A_n \sin(n\theta) + B_n \cos(n\theta)] + \sum_{n=-\infty}^{-1} r^n [C_n \sin(n\theta) + D_n \cos(n\theta)] \quad (8)$$

The expression was further simplified for the five modeled regions (*Griffiths, 1999*; *Ye et al., 2011*)

$$V_n = \left(\frac{A_n}{r} + C_n r\right)\sin\theta \tag{9}$$

where A_n, C_n were unknown coefficients ($n = 0, 1, 2, 3, 4$). These coefficients were solved in the Appendix (File S1), by considering boundary conditions (A–D). Substituting A_3, C_3 into (9), we obtained the expression of voltage inside the axolemma

$$V_3 = -\frac{8a^2b^2c^2E_0S_0S_1S_2\cos\theta}{r}\left[\frac{\text{term1}}{\text{term2} + \text{term3}}\right]. \tag{10}$$

where

$$\text{term1} = d^2(S_3 - S_4) + r^2(S_3 + S_4)$$

$$\begin{aligned}\text{term2} = {} & b^2(S_0 - S_1) \times \{c^2(S_1 + S_2)[d^2(S_2 + S_3)(S_3 - S_4) + c^2(S_2 - S_3)(S_3 + S_4)] \\ & + b^2(S_1 - S_2)[d^2(S_2 - S_3)(S_3 - S_4) + c^2(S_2 + S_3)(S_3 + S_4)]\}\end{aligned}$$

$$\begin{aligned}\text{term3} = {} & a^2(S_0 + S_1) \times \{c^2(S_1 - S_2)[d^2(S_2 + S_3)(S_3 - S_4) + c^2(S_2 - S_3)(S_3 + S_4)] \\ & + b^2(S_1 + S_2)[d^2(S_2 - S_3)(S_3 - S_4) + c^2(S_2 + S_3)(S_3 + S_4)]\}\end{aligned}$$

The axonal transmembrane potential (Vm) of the field was obtained by subtracting the membrane potential at the inner surface from that of the outer surface of the axon (*Kotnik, Bobanovic & Miklavcic, 1997*; *Kotnik & Miklavcic, 2000a*; *Ye et al., 2010*, *2011*), $V_m = V_3(r = d) - V_3(r = c)$. For a myelin-covered axon (File S2),

$$V_m = 8a^2b^2c(c - d)E_0S_0\left[\frac{\text{term4}}{\text{term2} + \text{term3}}\right]\cos\theta \tag{11}$$

Where

$$\text{term4} = S_1S_2[d(-S_3 + S_4) + c(S_3 + S_4)]$$

Voltage drop (Φ) across the myelin sheath was obtained by subtracting the myelin potential at the inner surface from the outer surface of the myelin (File S2)

$$\varnothing = 2a(a - b)E_0S_0\left[\frac{\text{term5} + \text{term6}}{\text{term2} + \text{term3}}\right]\cos\theta \tag{12}$$

Where

$$\begin{aligned}\text{term5} = {} & b\{c^2(S_1 + S_2) \times [d^2(S_2 + S_3)(-S_3 + S_4) - c^2(S_2 - S_3)(S_3 + S_4)] \\ & - b^2(S_1 - S_2)[d^2(S_2 - S_3)(S_3 - S_4) + c^2(S_2 + S_3)(S_3 + S_4)]\}\end{aligned}$$

$$\begin{aligned}\text{term6} = {} & a\{c^2(S_1 - S_2) \times [d^2(S_2 + S_3)(S_3 - S_4) + c^2(S_2 - S_3)(S_3 + S_4)] \\ & + b^2(S_1 + S_2)[d^2(S_2 - S_3)(S_3 - S_4) + c^2(S_2 + S_3)(S_3 + S_4)]\}\end{aligned}$$

Vm and Φ were functions of both field properties and tissue properties. The field properties included the orientation of the field and its intensity. The tissue properties include the electric parameters (conductivity and di-electricity) and the geometrical parameters (i.e., diameters of the axon). The above Vm expression for the myelin-covered axon (Eq. (11)) was further simplified for a bare axon by assuming $S_1 = S_0$ and $S_2 = S_0$ (File S3),

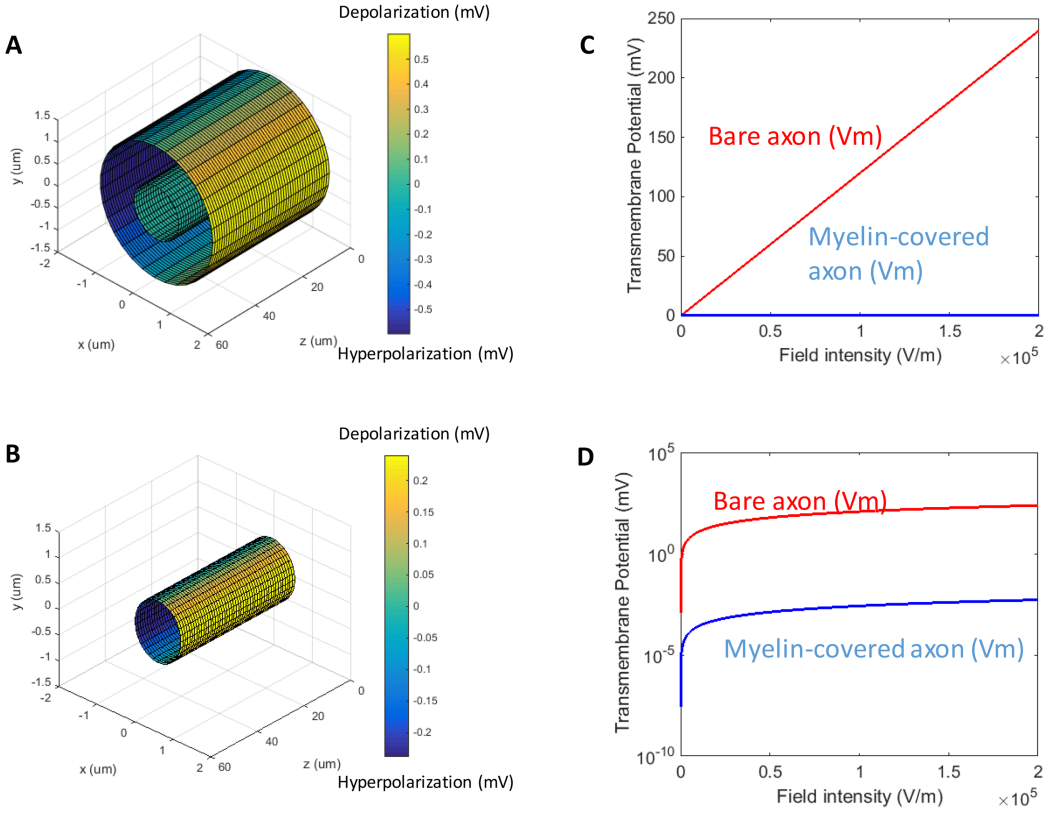

Figure 2 Polarization of a myelin-covered axon (A) and a bare axon (B) in a transverse electric field. The *Vm* was calculated by Eqs. (11) and (13), for the myelin-covered axon and the bare axon, respectively. ϕ was calculated by Eq. (12). All calculations were based on the standard parameters in Table 1. The color maps represented the amount of polarization (in mV). (C) Effect of transverse electric field intensity on axonal polarization in myelin-covered and bare axons. (D) Log plot of (C).

Full-size DOI: 10.7717/peerj.6020/fig-2

$$V_m = \frac{2c(c-d)E_0S_0[d(-S_3+S_4)+c(S_3+S_4)]}{d^2(S_0-S_3)(S_3-S_4)+c^2(S_0+S_3)(S_3+S_4)}\cos\theta \tag{13}$$

Impact of electric field properties on *Vm*

When a transverse electric field penetrates the axolemma, the geometrical pattern of *Vm* is determined by the axon's orientation to the electric field. The axolemma should be hyperpolarized wherever an electric current enters the membrane and be depolarized wherever the current extrudes from the membrane (*Ye & Steiger, 2015*). We plotted the transmembrane potential for a 50 μm myelinated axon (Fig. 2A) and a straight bare axon (Fig. 2B), based on the calculated *Vm* using standard values (Table 1). As expected, the locations of maximum polarization were at two lines corresponding to when θ = 180° (hyperpolarization, blue) and θ = 0° (depolarization, yellow), respectively. The axons were not polarized at the locations where θ = 90° and θ = 270°.

When the axon was wrapped by a thick myelin sheath, the geometrical pattern of the axolemma depolarization (Fig. 2A) remained identical to an unmyelinated axon

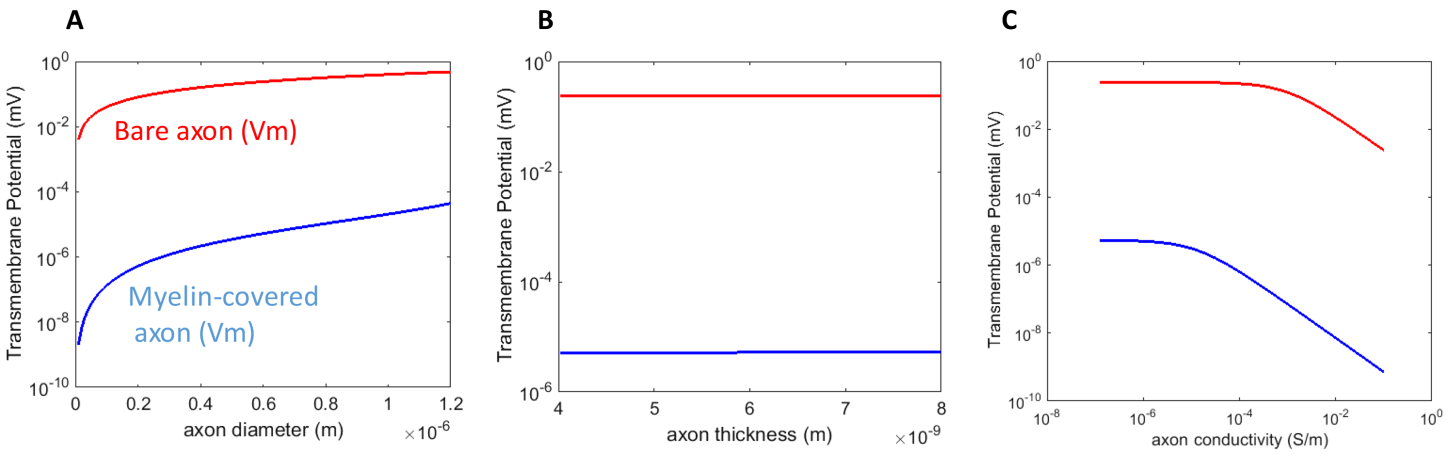

Figure 3 Dependency of *Vm* on the biophysics properties of the axon. (A) Axolemma diameter. (B) Axolemma thickness. (C) Axolemma conductivity.
Full-size DOI: 10.7717/peerj.6020/fig-3

(Fig. 2B). However, since a large voltage gradient (ϕ) was generated on the myelin sheath rather than on the axolemma, *Vm* was quantitatively negligible for the myelinated axon. With the standard values in Table 1, the maximum Φ was 0.6 mV for the myelin sheath, and the maximum *Vm* was only 0.53×10^{-2} μV for the axolemma. In contrast, when the axon was not myelinated, the maximum *Vm* was 0.24 mV.

For both the myelin-covered and bare axons, *Vm* was proportional to the intensity of the electric field (Figs. 2C and 2D). Two kV/cm was sufficient in inducing electroporation (*Sadik et al., 2011*). This intensity induced a *Vm* of 5.3 μV for the myelin-covered axon. For a bare axon, it induced a *Vm* of 239.9 mV, which is sufficient to break down the structure of the membrane (*Gehl, 2003*; *Kinosita & Tsong, 1977*). These results suggest that the myelin sheath could provide a "shielding effect" on the axolemma against field-induced excessive polarization and structure disruption.

Impact of axonal properties on *Vm*

We investigated the dependency of *Vm* on the axonal properties, including the geometrical features (axon radius and membrane thickness) of the axon, and its conductivity. For the parametric analysis, we plotted the maximum polarization ($\theta = 0^\circ$ on the axon surface, Figs. 1 and 2) when one parameter was varied through its defined value range, while the others were maintained at their standard values.

An axon with a larger radius was associated with a greater *Vm* for both the myelin-covered axon and bare axon (Fig. 3A) under a transverse field stimulation. Axon thickness, however, did not significantly affect *Vm* (Fig. 3B). *Vm* was insensitive to the axonal conductance changes within its physiological range (10^{-8}–10^{-6} S/m), in agreement with the literature that studied spherical cell polarization in an electric field (*Kotnik, Bobanovic & Miklavcic, 1997*; *Kotnik & Miklavcic, 2006*). However, when axolemma conductivity was significantly increased (>10^{-3} S/m) due to membrane disruption and leakage, such as during electroporation (*Mossop et al., 2004*, *2007*),

axolemma depolarization decreased significantly for both the myelin-covered and bare axons (Fig. 3C).

Impact of demyelination on axonal *Vm*

Myelin, like a neuronal cell membrane, is constructed of a lipid bilayer that contains a hydrophobic center and hydrophilic surface. Myelin wraps around an axon numerous times, each layer acting like multiple resistors in series. Demyelination occurs in many neurological diseases such as spinal cord injury (*Ye et al., 2012*), cerebral palsy (*Ruff et al., 2013*) and multiple sclerosis (*Lazzarini, 2004*). Demyelination is defined by the significant loss of myelin thickness (*Mainero et al., 2015*; *Manogaran et al., 2016*) and increased conductivity of the myelin.

We first studied how the loss of myelin layers could affect *Vm* in a transverse electric field. We systematically decreased the myelin thickness from 4.0–0.1 μm. The conductivity of the myelin increased linearly with the reduction of the myelin thickness. This caused a reduction in the potential drop across the myelin sheath, but it did not significantly affect axonal depolarization (Fig. 4). The transverse electric field was ineffective in inducing axonal depolarization, assuming the remaining myelin sheath could maintain low conductivity (~10^{-7} S/m).

We then investigated how an increase of myelin conductivity could affect *Vm* in a transverse electric field. When myelin conductivity was as low as 5×10^{-5} S/m, reduction in myelin thickness did not lead to dramatic changes in *Vm* (Fig. 5A). Instead, it led to a voltage drop across the myelin sheath (Φ). When myelin conductivity was increased to 5×10^{-3} S/m, *Vm* could exceed ϕ for an extremely thin myelin sheath (Fig. 5B). For a very leaky myelin (myelin conductivity is 5×10^{-1} S/m), the axon could be significantly depolarized at any myelin thickness (Fig. 5C), and *Vm* could be greater than Φ for a thin myelin sheath (Fig. 5D). However, Φ still dominated for axons with thick myelin sheaths (Fig. 5E). In conclusion, demyelination could cause a re-distribution of the potentials between the axolemma and myelin under transverse electric stimulation. Increases in myelin conductivity during demyelination could cause the voltage distribution to shift from the myelin sheath to the axon. Axonal depolarization became prominent when significant reduction of myelin conductivity occurred during demyelination.

DISCUSSION

This work provides a novel analytical expression that describes the membrane polarization of axons (myelinated and bare) under transverse field stimulation. It analyzes the biophysical factors that affect axonal polarization under physiological conditions, and under pathological conditions such as demyelination. Finally, it provides the needed term to modify the current cable equation, so that the equation can account for the effects of more realistic field, which include both the transverse and parallel directions.

Impact of field orientation on *Vm* in transverse current stimulation

The model shows that the longitudinal axon was polarized with a distinct geometrical pattern by the transverse electric field, which was dependent on the orientation of the axon

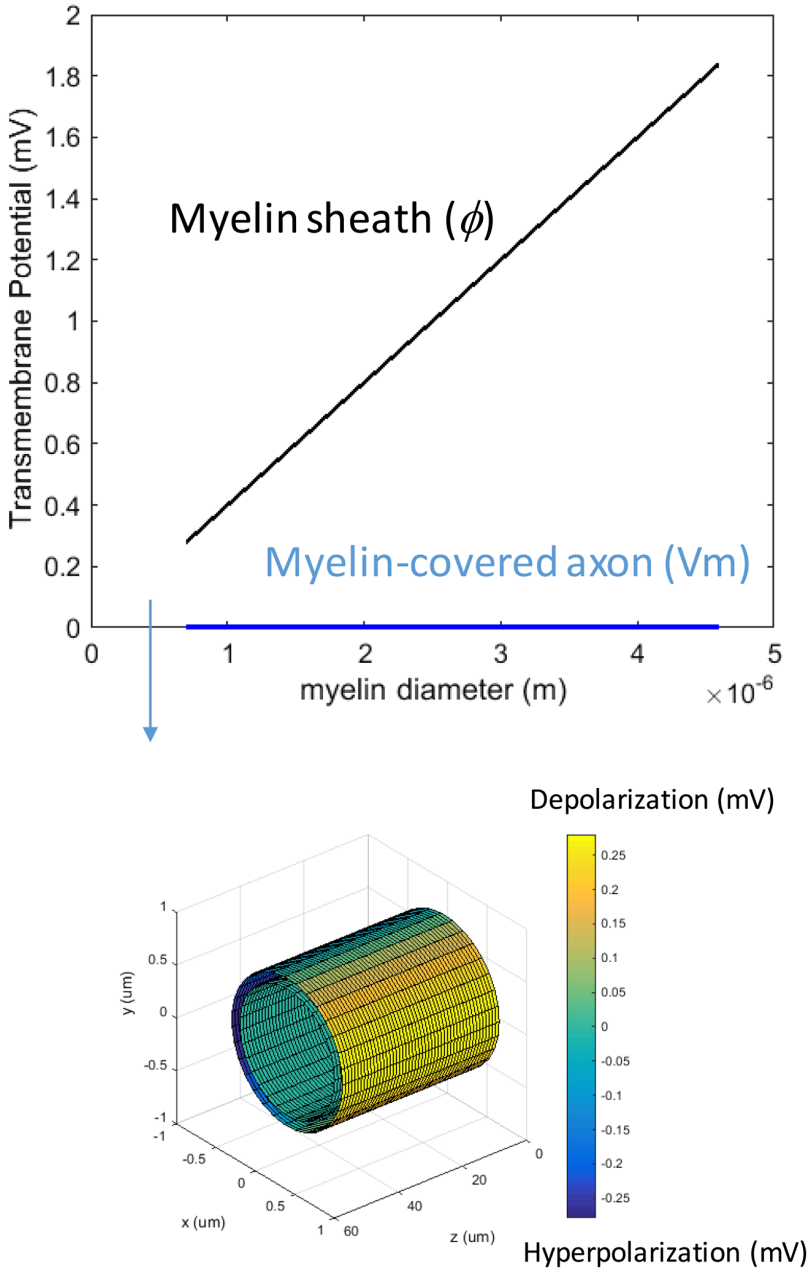

Figure 4 Effects of decreased myelin thickness on axonal polarization. Reduction of myelin thickness from 3.4 to 0.1 µm (and linear increase of its conductivity) caused a significant reduction in ϕ, but not *Vm*. For the inset example, axon diameter = 0.6 µm. Myelin thickness = 0.1 µm.

Full-size DOI: 10.7717/peerj.6020/fig-4

in the field. Previously, regional polarization has been observed in a variety of modeling and experimental studies for cells under electric (*Durand, 2003*; *Lee & Grill, 2005*; *Lu et al., 2008*; *Teruel & Meyer, 1997*) and magnetic field stimulation (*Schnabel & Struijk, 1999*, *2001*; *Ye, Cotic & Carlen, 2007*). Functionally, orientation of the electric field to the axon is important for the excitation of axons, such as those from the retina ganglion cells (*Grumet, Wyatt & Rizzo, 2000*). Since only a small patch of membrane is depolarized

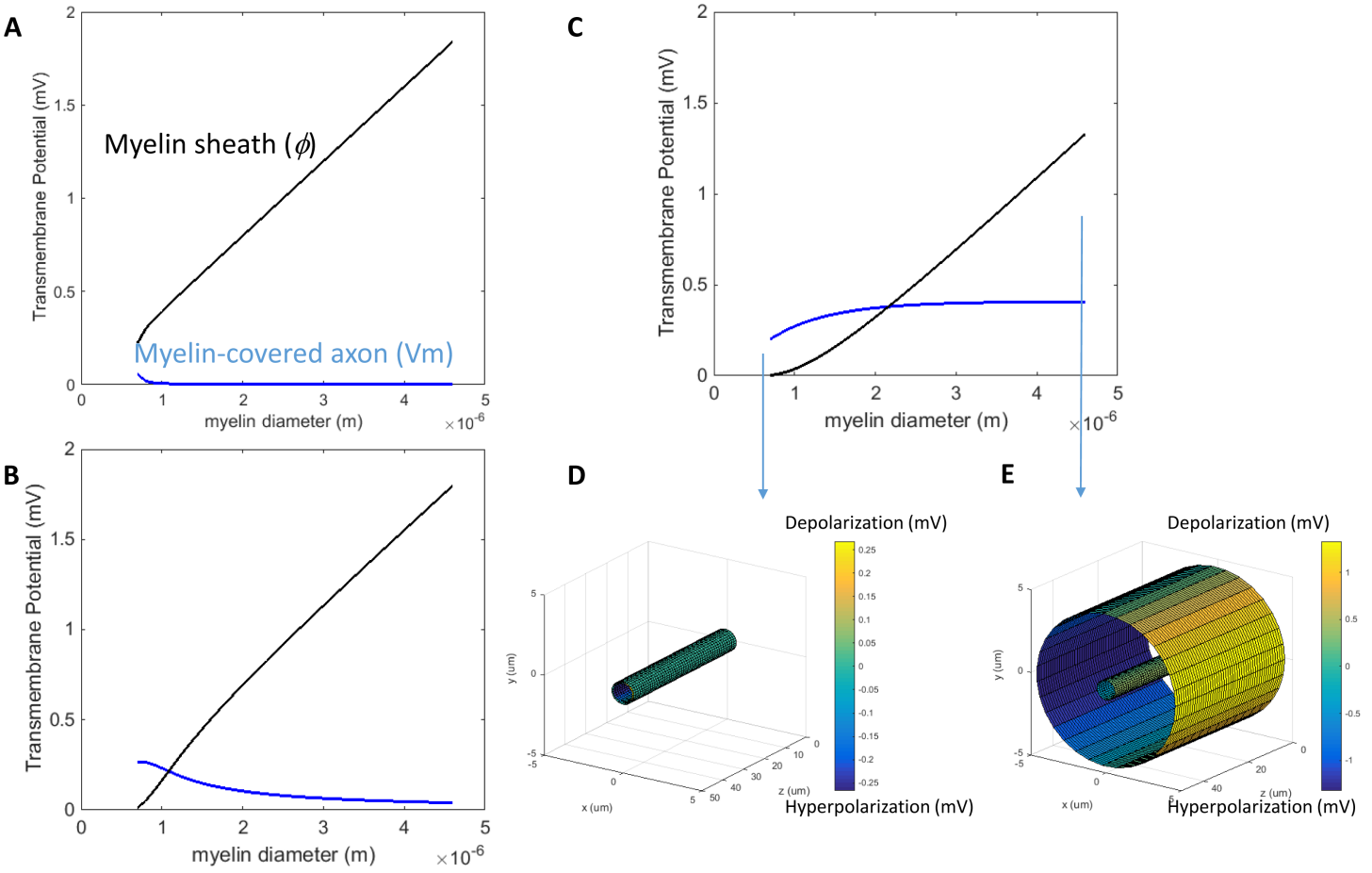

Figure 5 Effects of a leaky myelin sheath on axolemma polarization in a transverse electric field. Conductivity of each myelin layer was (A) 5×10^{-5} S/m, (B) 5×10^{-3} S/m, and (C) 5×10^{-1} S/m, respectively. (D) Example of axon polarization when axon diameter = 0.6 µm and myelin diameter = 0.7 µm. (E) Example of axon polarization when axon diameter = 0.6 µm and myelin diameter = 4.6 µm.

Full-size DOI: 10.7717/peerj.6020/fig-5

in the transverse field, it is reasonable to speculate that voltage gated ion channels may have a diverse response to the field, depending on their location on the membrane patch. This could cause the threshold for activation to be higher than that observed from axons in longitudinal fields that induce the same peak depolarization (*Schnabel & Struijk, 2001*). The higher threshold may explain the relative poor efficiency of axonal activation by transverse field stimulation (*McNeal, 1976*; *Ranck, 1975*).

Impact of axon's biophysical properties on *Vm*

We found that *Vm* was dependent on the intrinsic tissue properties of an axon. We observed that *Vm* was greater in larger diameter axons than in smaller ones (Fig. 3A). This observation is in agreement with the notion that larger diameter axons are associated with lower excitation thresholds (*Basser & Roth, 1991*; *Carbunaru & Durand, 1997*; *Garnsworthy et al., 1988*; *Reilly, 1989*). Selective activation of different size fibers has significant clinical implications, such as pain relief (*Meyerson & Linderoth, 2000*), which can be achieved by novel design of the electric field (*Konings, 2007*). In deep brain

stimulation, the effects of the electric currents within different brain regions were dependent on the fiber sizes (*Sotiropoulos & Steinmetz, 2007*). In addition, an increase in axolemma conductivity decreases the axon's sensitivity (buildup of *Vm*) to the transverse field (Fig. 3C), suggesting a shunting effect to the transverse current. In conclusion, the effectiveness of transverse stimulation relies on the physiological features of the target axon.

Axonal diameter could change under certain pathological situations. For example, axon swelling occurs during focal demyelination (*Kolaric et al., 2013*), as a consequence of aglycemia (*Allen et al., 2006*), anoxia (*Waxman et al., 1992*) or ischemia (*Garthwaite et al., 1999*). It is speculated that these pathological changes could potentially render the enlarged axons more sensitive to the transverse electric field.

Impact of demyelination and other pathological conditions on *Vm* in transverse electric stimulation

Dynamic changes of myelin occur during demyelination. It is unknown if pathological demyelination could affect the sensitivity of a myelinated axon to a transverse electric field. While myelin-covered axons could only be slightly depolarized by the transverse field, bare axons can have a moderate buildup of *Vm* (Fig. 2), especially when the axon diameter is large (Fig. 5A). We used the model to test two possibilities of reduced myelination and their impacts on *Vm*. Reduction in the myelin thickness, along with a scaled linear increase in myelin conductance, was not sufficient to enhance depolarization (Fig. 4). In contrast, *Vm* was enhanced when the myelin sheath became electrically leaky (highly conductive) (Fig. 5). It is therefore expected that transverse electric fields could apply variable axonal depolarization, depending on the myelin conductivity changes during the process of demyelination. Electrical stimulation protocols for the treatment of demyelination diseases (*Dooley & Sharkey, 1981*; *Dooley et al., 1978*) could be further optimized by considering remyelination/demyelination factors during treatment, to ensure maximum outcomes.

Dynamic changes of myelin also occur during development (*Sturrock, 1980*), neural regeneration (*Huang et al., 2013*), and pathological situations such as traumatic brain injury (*Robain & Mandel, 1974*; *Tyler, 2012*). At the cellular level, membrane resistance of the oligodendrocyte could change during development and maturity (*Karadottir et al., 2005*), and in a medium with low osmolarity (*Kimelberg & Kettenmann, 1990*). It is speculated that these dynamic changes in the myelin properties could cause the axons to react differently to the electric field. This supports the notion that the dynamic interaction between the electric field and the neuronal tissue, as well as the outcome of the stimulation, are determined by both the electric parameters and the tissue properties (*Ye & Steiger, 2015*).

Modification of the cable equation to include the transverse field

The analytical expression of the *Vm* term could potentially be used to modify the current cable equation to account for both $E_{//}$ and $E_{\perp}$. *Ruohonen et al. (1996)* modified the cable equation to be in the form of $\lambda^2 \frac{\partial^2 \phi_m}{\partial x^2} - \tau \frac{\partial \phi_m}{\partial t} - \phi_m - 2c(\alpha E'_{//} - E_{\perp}) = 0$.

Here, $\alpha E'_{//} - E_{\perp}$ is interpreted as the *modified activating function*, where $\alpha = \frac{\lambda^2}{2c} = \frac{R_m}{4R_i}$ (*Ruohonen et al., 1996*). Comparatively large values of α indicates that $E'_{//}$ is responsible for the majority of excitation, while $\alpha = 0$ indicates that $E_{\perp}$ is more important.

In this modified equation, the term $2cE_{\perp}$ is the membrane potential created by the transverse field. For magnetic stimulation, an analytical expression (*Ye et al., 2011*) is available to replace this term for the modified cable equation. For direct electric stimulation, the *Vm* term for the unmyelinated axon (Eq. (13)) can be used to replace the $2cE\perp$ term, to include the impact of the transverse electric field. Previously, effects of the transverse field and the axial field have been compared in several works (*Lontis, Nielsen & Struijk, 2009*; *Ruohonen et al., 1996*; *Yu, Zheng & Wang, 2005*). The transverse electric field is required to be several times greater than the longitudinal field to produce comparable results (*McNeal, 1976*; *Ranck, 1975*; *Ruohonen et al., 1996*). A precondition for the modified activation function to yield accurate results is for the electric field to be approximately uniform and be perpendicular to the axon fiber (*Schnabel & Struijk, 2001*), which is readily satisfied in our model.

Limitations and future directions

This paper was not intended to fully elucidate the mechanisms behind transverse field activation of nerve tissue, since it did not include any ionic channel mechanisms. The model also does not necessarily apply to the stimulation of fiber bundles. Axons within a bundle could interfere with other axon's polarization under a transverse electric field (*Pourtaheri et al., 2009*). Local electric fields could be perturbed by an axon, which produces a small, secondary effect on the surrounding axons (*Lee & Grill, 2005*; *Susil, Semrov & Miklavcic, 1998*). In a nerve bundle, *Vm* could also be a function of the anisotropy of the bundle (*Nagarajan & Durand, 1995*), which was not studied in the present model. Finally, the transverse field could be significantly weaker due to the lower values of conductance of surrounding perineurium (*Struijk & Schnabel, 2001*). More complicated modeling work should resort to numerical methods, whose accuracy can be validated by the analytical results from this work.

The model predicts that the node section in a myelinated axon will have the same polarization as the unmyelinated axon. If one considers that the node has a much higher density of Na^+ channel distribution (*Freeman et al., 2016*), it is predicted that myelinated axons will have a lower threshold of activation under transverse electric field. This model prediction could be tested by stimulating a structure that contains both unmyelinated and myelinated axons, such as the corpus callosum (*Crawford, Mangiardi & Tiwari-Woodruff, 2009*; *Ruff et al., 2013*). With the strong stimulus being applied on both type of axons (*Ruff et al., 2013*), action potentials should be triggered first in the myelinated axons.

CONCLUSIONS

This work provides novel analytical expressions of the electrically-induced transmembrane potential (*Vm*) for a myelin-covered axon and a bare, unmyelinated axon, under a transverse DC electric field. Results show that the myelin sheath shields the axon from extensive depolarization. Demyelination could alter axon's sensitivity to a transverse electric field if the process of demyelination involves significant increases in the electric

conductance of the myelin. The analytical solution of *Vm* for the unmyelinated axon can be used to improve the activation function of the current cable equation that describes electric stimulation.

APPENDIX—DETERMINING UNKNOWN COEFFICIENTS A_n, C_n IN EQ. (9) USING BOUNDARY CONDITIONS (A–D)

At an infinite distance, according to boundary condition (C), $V_o = -E_0 r\cos\theta$. Therefore, $a_0 = -E_0$. Since V was bounded at $r = 0$ (boundary condition D), $C_4 = 0$.

Expressions for the potential distribution in the five modeled regions were:

$$V_0 = -E_0 r\cos\theta + \frac{C_0}{r}\cos\theta \tag{A-1}$$

$$V_1 = A_1 r\cos\theta + \frac{C_1}{r}\cos\theta \tag{A-2}$$

$$V_2 = A_2 r\cos\theta + \frac{C_2}{r}\cos\theta \tag{A-3}$$

$$V_3 = A_3 r\cos\theta + \frac{C_3}{r}\cos\theta \tag{A-4}$$

$$V_4 = A_4 r\cos\theta \tag{A-5}$$

The $\vec{r}$ components of ∇V (from Eq. (1)) were continuous across the interfaces (boundary condition A), and the normal components of the current density were continuous across the interfaces (boundary condition B). These boundary conditions yield the following set of equations:

On the #0#1 interface (r = a)

$$-E_0 a + \frac{C_0}{a} = aA_1 + \frac{C_1}{a} \tag{A-6}$$

$$S_0\left(-E_0 - \frac{C_0}{a^2}\right) = S_1\left(A_1 - \frac{C_{11}}{a^2}\right) \tag{A-7}$$

On the #1#2 interface (r = b)

$$bA_1 + \frac{C_1}{b} = bA_2 + \frac{C_2}{b} \tag{A-8}$$

$$S_1\left(A_1 - \frac{C_1}{b^2}\right) = S_2\left(A_2 - \frac{C_2}{b^2}\right) \tag{A-9}$$

On the #2#3 interface (r = c)

$$cA_2 + \frac{C_2}{c} = cA_3 + \frac{C_3}{c} \tag{A-10}$$

$$S_2\left(A_2 - \frac{C_2}{c^2}\right) = S_3\left(A_3 - \frac{C_3}{c^2}\right) \tag{A-11}$$

On the #3#4 interface (r = d)

$$dA_3 + \frac{C_3}{d} = dA_4 \tag{A-12}$$

$$S_3\left(A_3 - \frac{C_3}{d^2}\right) = S_4 A_4 \tag{A-13}$$

We solved (A-6) to (A-13) to obtain the unknown coefficients (File S1). These coefficients will be substituted into (A-1) to (A-5) to obtain the analytical expression of the voltages in the five regions (File S1).

LIST OF ABBREVIATIONS

DC	Direct current
$\boldsymbol{E_0}$	Intensity of the externally applied DC electric field (V/m)
Vm	Transmembrane potential induced by the DC electric field across the axolemma (mV)
ϕ	Potential drop across the myelin sheath (mV)
$\boldsymbol{E_{//}}$	Electric field that is parallel to the axon
$\boldsymbol{E_{\perp}}$	Electric field that is perpendicular (traversal) to the axon.

ACKNOWLEDGEMENTS

The authors thanks Austen Curcuru for the assistance in deriving the equations.

ADDITIONAL INFORMATION AND DECLARATIONS

Funding

The authors received no funding for this work.

Competing Interests

The authors declare that they have no competing interests.

Author Contributions

- Hui Ye conceived and designed the experiments, performed the experiments, analyzed the data, contributed reagents/materials/analysis tools, prepared figures and/or tables, authored or reviewed drafts of the paper, approved the final draft.
- Jeffrey Ng authored or reviewed drafts of the paper, approved the final draft, paper revision.

Data Availability

The following information was supplied regarding data availability:

The raw data are provided in the Supplemental Files.

Supplemental Information

Supplemental information for this article can be found online at http://dx.doi.org/10.7717/peerj.6020#supplemental-information.

REFERENCES

Allen L, Anderson S, Wender R, Meakin P, Ransom BR, Ray DE, Brown AM. 2006. Fructose supports energy metabolism of some, but not all, axons in adult mouse optic nerve. *Journal of Neurophysiology* **95(3)**:1917–1925 DOI 10.1152/jn.00637.2005.

Amassian VE, Maccabee PJ, Cracco RQ. 1989. Focal stimulation of human peripheral nerve with the magnetic coil: a comparison with electrical stimulation. *Experimental Neurology* **103(3)**:282–289 DOI 10.1016/0014-4886(89)90052-6.

Bakiri Y, Karadottir R, Cossell L, Attwell D. 2011. Morphological and electrical properties of oligodendrocytes in the white matter of the corpus callosum and cerebellum. *Journal of Physiology* **589(3)**:559–573 DOI 10.1113/jphysiol.2010.201376.

Basser PJ, Roth BJ. 1991. Stimulation of a myelinated nerve axon by electromagnetic induction. *Medical & Biological Engineering & Computing* **29(3)**:261–268 DOI 10.1007/bf02446708.

Basser PJ, Roth BJ. 2000. New currents in electrical stimulation of excitable tissues. *Annual Review of Biomedical Engineering* **2(1)**:377–397 DOI 10.1146/annurev.bioeng.2.1.377.

Basser PJ, Wijesinghe RS, Roth BJ. 1992. The activating function for magnetic stimulation derived from a three-dimensional volume conductor model. *IEEE Transactions on Biomedical Engineering* **39(11)**:1207–1210 DOI 10.1109/10.168686.

Berthold CH, Nilsson I, Rydmark M. 1983. Axon diameter and myelin sheath thickness in nerve fibres of the ventral spinal root of the seventh lumbar nerve of the adult and developing cat. *Journal of Anatomy* **136**:483–508.

Berthold CH, Rydmark M. 1995. Morphology of normal peripheral axon. In: Waxman SG, Kocsis JD, Stys PK, eds. *The Axon: Structure, Function, and Pathophysiology*. New York: Oxford University Press, 13–48.

Bikson M, Lian J, Hahn PJ, Stacey WC, Sciortino C, Durand DM. 2001. Suppression of epileptiform activity by high frequency sinusoidal fields in rat hippocampal slices. *Journal of Physiology* **531(1)**:181–191 DOI 10.1111/j.1469-7793.2001.0181j.x.

Bingham RJ, Olmsted PD, Smye SW. 2010. Undulation instability in a bilayer lipid membrane due to electric field interaction with lipid dipoles. *Physical Review E* **81(5)**:051909 DOI 10.1103/PhysRevE.81.051909.

Carbunaru R, Durand DM. 1997. Axonal stimulation under MRI magnetic field z gradients: a modeling study. *Magnetic Resonance in Medicine* **38(5)**:750–758 DOI 10.1002/mrm.1910380511.

Chomiak T, Hu B. 2009. What is the optimal value of the g-ratio for myelinated fibers in the rat CNS? A theoretical approach. *PLOS ONE* **4(11)**:e7754 DOI 10.1371/journal.pone.0007754.

Coderre TJ, Katz J, Vaccarino AL, Melzack R. 1993. Contribution of central neuroplasticity to pathological pain: review of clinical and experimental evidence. *Pain* **52(3)**:259–285 DOI 10.1016/0304-3959(93)90161-h.

Cranford JP, Kim BJ, Neu WK. 2012. Asymptotic model of electrical stimulation of nerve fibers. *Medical & Biological Engineering & Computing* **50(3)**:243–251 DOI 10.1007/s11517-012-0870-3.

Crawford DK, Mangiardi M, Tiwari-Woodruff SK. 2009. Assaying the functional effects of demyelination and remyelination: revisiting field potential recordings. *Journal of Neuroscience Methods* **182(1)**:25–33 DOI 10.1016/j.jneumeth.2009.05.013.

Cros D, Day TJ, Shahani BT. 1990. Spatial dispersion of magnetic stimulation in peripheral nerves. *Muscle & Nerve* **13(11)**:1076–1082 DOI 10.1002/mus.880131110.

Dooley DM, Sharkey J. 1981. Electrical stimulation of the spinal cord in patients with demyelinating and degenerative diseases of the central nervous system. *Applied Neurophysiology* **44(4)**:218–224 DOI 10.1159/000102204.

Dooley DM, Sharkey J, Keller W, Kasprak M. 1978. Treatment of demyelinating and degenerative diseases by electro stimulation of the spinal cord. *Medical Progress through Technology* **6**:1–14.

Durand DM. 2003. Electric field effects in hyperexcitable neural tissue: a review. *Radiation Protection Dosimetry* **106(4)**:325–331 DOI 10.1093/oxfordjournals.rpd.a006368.

Esselle KP, Stuchly MA. 1994. Quasi-static electric field in a cylindrical volume conductor induced by external coils [human body application]. *IEEE Transactions on Biomedical Engineering* **41(2)**:151–158 DOI 10.1109/10.284926.

Esselle KP, Stuchly MA. 1995. Cylindrical tissue model for magnetic field stimulation of neurons: effects of coil geometry. *IEEE Transactions on Biomedical Engineering* **42(9)**:934–941 DOI 10.1109/10.412660.

Farkas DL, Korenstein R, Malkin S. 1984. Electrophotoluminescence and the electrical properties of the photosynthetic membrane. I. Initial kinetics and the charging capacitance of the membrane. *Biophysical Journal* **45(2)**:363–373 DOI 10.1016/S0006-3495(84)84160-0.

Freeman SA, Desmazieres A, Fricker D, Lubetzki C, Sol-Foulon N. 2016. Mechanisms of sodium channel clustering and its influence on axonal impulse conduction. *Cellular and Molecular Life Sciences* **73(4)**:723–735 DOI 10.1007/s00018-015-2081-1.

Fricke H. 1953. The electric permittivity of a dilute suspension of membrane-covered ellipsoids. *Journal of Applied Physics* **24(5)**:644–646 DOI 10.1063/1.1721343.

Galvani A. 1791. De viribus electricitatis in motu musculari commentaries. *Bononiensi Scientiarum et Artium Instituto atque Academia Commentarii* **7**:363–418.

Garnsworthy RK, Gully RL, Kenins P, Westerman RA. 1988. Transcutaneous electrical stimulation and the sensation of prickle. *Journal of Neurophysiology* **59(4)**:1116–1127 DOI 10.1152/jn.1988.59.4.1116.

Garthwaite G, Brown G, Batchelor AM, Goodwin DA, Garthwaite J. 1999. Mechanisms of ischaemic damage to central white matter axons: a quantitative histological analysis using rat optic nerve. *Neuroscience* **94(4)**:1219–1230 DOI 10.1016/s0306-4522(99)00389-9.

Gehl J. 2003. Electroporation: theory and methods, perspectives for drug delivery, gene therapy and research. *Acta Physiologica Scandinavica* **177(4)**:437–447 DOI 10.1046/j.1365-201X.2003.01093.x.

Gimsa J, Wachner D. 2001. Analytical description of the transmembrane voltage induced on arbitrarily oriented ellipsoidal and cylindrical cells. *Biophysical Journal* **81(4)**:1888–1896 DOI 10.1016/S0006-3495(01)75840-7.

Griffiths DJ. 1999. *Introduction to Electrodynamics*. 3rd Edition. Upper Saddle River: Prentice Hall.

Grill WM, Wei XF. 2009. High efficiency electrodes for deep brain stimulation. *2009 Annual International Conference of the IEEE Engineering in Medicine and Biology Society*. Minneapolis: IEEE, 3298–3301.

Grumet AE, Wyatt JL Jr, Rizzo JF 3rd. 2000. Multi-electrode stimulation and recording in the isolated retina. *Journal of Neuroscience Methods* **101(1)**:31–42 DOI 10.1016/s0165-0270(00)00246-6.

Huang J, Zhang Y, Lu L, Hu X, Luo Z. 2013. Electrical stimulation accelerates nerve regeneration and functional recovery in delayed peripheral nerve injury in rats. *European Journal of Neuroscience* **38(12)**:3691–3701 DOI 10.1111/ejn.12370.

Jerry RA, Popel AS, Brownell WE. 1996. Potential distribution for a spheroidal cell having a conductive membrane in an electric field. *IEEE Transactions on Biomedical Engineering* **43(9)**:970–972 DOI 10.1109/10.532132.

Karadottir R, Cavelier P, Bergersen LH, Attwell D. 2005. NMDA receptors are expressed in oligodendrocytes and activated in ischaemia. *Nature* **438(7071)**:1162–1166 DOI 10.1038/nature04302.

Kimelberg HK, Kettenmann H. 1990. Swelling-induced changes in electrophysiological properties of cultured astrocytes and oligodendrocytes. I. Effects on membrane potentials, input impedance and cell-cell coupling. *Brain Research* **529(1–2)**:255–261 DOI 10.1016/0006-8993(90)90835-y.

Kinosita K Jr, Tsong TY. 1977. Voltage-induced pore formation and hemolysis of human erythrocytes. *Biochimica et Biophysica Acta—Biomembranes* **471(2)**:227–242 DOI 10.1016/0005-2736(77)90252-8.

Kolaric KV, Thomson G, Edgar JM, Brown AM. 2013. Focal axonal swellings and associated ultrastructural changes attenuate conduction velocity in central nervous system axons: a computer modeling study. *Physiological Reports* **1(3)**:e00059 DOI 10.1002/phy2.59.

Konings MK. 2007. A new method for spatially selective, non-invasive activation of neurons: concept and computer simulation. *Medical & Biological Engineering & Computing* **45(1)**:7–24 DOI 10.1007/s11517-006-0136-z.

Kotnik T, Bobanovic F, Miklavcic D. 1997. Sensitivity of transmembrane voltage induced by applied electric fields—a theoretical analysis. *Bioelectrochemistry and Bioenergetics* **43(2)**:285–291 DOI 10.1016/s0302-4598(97)00023-8.

Kotnik T, Miklavcic D. 2000a. Analytical description of transmembrane voltage induced by electric fields on spheroidal cells. *Biophysical Journal* **79(2)**:670–679 DOI 10.1016/S0006-3495(00)76325-9.

Kotnik T, Miklavcic D. 2000b. Second-order model of membrane electric field induced by alternating external electric fields. *IEEE Transactions on Biomedical Engineering* **47(8)**:1074–1081 DOI 10.1109/10.855935.

Kotnik T, Miklavcic D. 2006. Theoretical evaluation of voltage inducement on internal membranes of biological cells exposed to electric fields. *Biophysical Journal* **90(2)**:480–491 DOI 10.1529/biophysj.105.070771.

Kotnik T, Miklavcic D, Slivnik T. 1998. Time course of transmembrane voltage induced by time-varying electric field—a method for theoretical analysis and its application. *Bioelectrochemistry and Bioenergetics* **45(1)**:3–16 DOI 10.1016/s0302-4598(97)00093-7.

Krassowska W, Neu JC. 1994. Response of a single cell to an external electric field. *Biophysical Journal* **66(6)**:1768–1776 DOI 10.1016/S0006-3495(94)80971-3.

Lazzarini RA. 2004. *Myelin biology and disorders*. San Diego: Elsevier Academic.

Lee DC, Grill WM. 2005. Polarization of a spherical cell in a nonuniform extracellular electric field. *Annals of Biomedical Engineering* **33(5)**:603–615 DOI 10.1007/s10439-005-2397-3.

Lontis ER, Nielsen K, Struijk JJ. 2009. In vitro magnetic stimulation of pig phrenic nerve with transverse and longitudinal induced electric fields: analysis of the stimulation site. *IEEE Transactions on Biomedical Engineering* **56(2)**:500–512 DOI 10.1109/TBME.2008.2009929.

Lu H, Chestek CA, Shaw KM, Chiel HJ. 2008. Selective extracellular stimulation of individual neurons in ganglia. *Journal of Neural Engineering* **5(3)**:287–309 DOI 10.1088/1741-2560/5/3/003.

Maccabee PJ, Amassian VE, Cracco RQ, Eberle LP, Rudell AP. 1991. Mechanisms of peripheral nervous system stimulation using the magnetic coil. *Electroencephalography and Clinical Neurophysiology Supplement* **43**:344–361.

Maccabee PJ, Amassian VE, Eberle LP, Cracco RQ. 1993. Magnetic coil stimulation of straight and bent amphibian and mammalian peripheral nerve in vitro: locus of excitation. *Journal of Physiology* **460(1)**:201–219 DOI 10.1113/jphysiol.1993.sp019467.

Mainero C, Louapre C, Govindarajan ST, Gianni C, Nielsen AS, Cohen-Adad J, Sloane J, Kinkel RP. 2015. A gradient in cortical pathology in multiple sclerosis by in vivo quantitative 7 T imaging. *Brain* **138(4)**:932–945 DOI 10.1093/brain/awv011.

Manogaran P, Vavasour IM, Lange AP, Zhao Y, McMullen K, Rauscher A, Carruthers R, Li DK, Traboulsee AL, Kolind SH. 2016. Quantifying visual pathway axonal and myelin loss in multiple sclerosis and neuromyelitis optica. *NeuroImage: Clinical* **11**:743–750 DOI 10.1016/j.nicl.2016.05.014.

McNeal DR. 1976. Analysis of a model for excitation of myelinated nerve. *IEEE Transactions on Biomedical Engineering BME* **23(4)**:329–337 DOI 10.1109/tbme.1976.324593.

Meyerson BA, Linderoth B. 2000. Mechanisms of spinal cord stimulation in neuropathic pain. *Neurological Research* **22**:285–292.

Mossop BJ, Barr RC, Henshaw JW, Yuan F. 2007. Electric fields around and within single cells during electroporation—a model study. *Annals of Biomedical Engineering* **35(7)**:1264–1275 DOI 10.1007/s10439-007-9282-1.

Mossop BJ, Barr RC, Zaharoff DA, Yuan F. 2004. Electric fields within cells as a function of membrane resistivity—a model study. *IEEE Transactions on Nanobioscience* **3(3)**:225–231 DOI 10.1109/tnb.2004.833703.

Nagarajan SS, Durand DM. 1995. Analysis of magnetic stimulation of a concentric axon in a nerve bundle. *IEEE Transactions on Biomedical Engineering* **42(9)**:926–933 DOI 10.1109/10.412659.

Nowak LG, Bullier J. 1998. Axons, but not cell bodies, are activated by electrical stimulation in cortical gray matter I. Evidence from chronaxie measurements. *Experimental Brain Research* **118(4)**:477–488 DOI 10.1007/s002210050304.

Olney RK, So YT, Goodin DS, Aminoff MJ. 1990. A comparison of magnetic and electrical stimulation of peripheral nerves. *Muscle & Nerve* **13(10)**:957–963 DOI 10.1002/mus.880131012.

Polk C, Song JH. 1990. Electric fields induced by low frequency magnetic fields in inhomogeneous biological structures that are surrounded by an electric insulator. *Bioelectromagnetics* **11(3)**:235–249 DOI 10.1002/bem.2250110305.

Pourtaheri N, Ying W, Kim JM, Henriquez CS. 2009. Thresholds for transverse stimulation: fiber bundles in a uniform field. *IEEE Transactions on Neural Systems and Rehabilitation Engineering* **17(5)**:478–486 DOI 10.1109/TNSRE.2009.2033424.

Ranck JB Jr. 1975. Which elements are excited in electrical stimulation of mammalian central nervous system: a review. *Brain Research* **98(3)**:417–440 DOI 10.1016/0006-8993(75)90364-9.

Ravazzani P, Ruohonen J, Grandori F, Tognola G. 1996. Magnetic stimulation of the nervous system: induced electric field in unbounded, semi-infinite, spherical, and cylindrical media. *Annals of Biomedical Engineering* **24(5)**:606–616 DOI 10.1007/bf02684229.

Reilly JP. 1989. Peripheral nerve stimulation by induced electric currents: exposure to time-varying magnetic fields. *Medical & Biological Engineering & Computing* **27(2)**:101–110 DOI 10.1007/bf02446217.

Robain O, Mandel P. 1974. Quantitative study of myelination and axonal growth in corpus callosum and posterior columns of spinal cord in the Jimpy mouse (author's transl). *Acta Neuropathologica* **29**:293–309.

Roth BJ, Basser PJ. 1990. A model of the stimulation of a nerve fiber by electromagnetic induction. *IEEE Transactions on Biomedical Engineering* **37(6)**:588–597 DOI 10.1109/10.55662.

Roth BJ, Cohen LG, Hallett M, Friauf W, Basser PJ. 1990. A theoretical calculation of the electric field induced by magnetic stimulation of a peripheral nerve. *Muscle & Nerve* **13(8)**:734–741 DOI 10.1002/mus.880130812.

Ruff CA, Ye H, Legasto JM, Stribbell NA, Wang J, Zhang L, Fehlings MG. 2013. Effects of adult neural precursor-derived myelination on axonal function in the perinatal congenitally dysmyelinated brain: optimizing time of intervention, developing accurate prediction models, and enhancing performance. *Journal of Neuroscience* **33(29)**:11899–11915 DOI 10.1523/jneurosci.1131-13.2013.

Ruohonen J, Panizza M, Nilsson J, Ravazzani P, Grandori F, Tognola G. 1996. Transverse-field activation mechanism in magnetic stimulation of peripheral nerves. *Electroencephalography and Clinical Neurophysiology/Electromyography and Motor Control* **101(2)**:167–174 DOI 10.1016/0924-980x(95)00237-f.

Sadik MM, Li J, Shan JW, Shreiber DI, Lin H. 2011. Vesicle deformation and poration under strong dc electric fields. *Physical Review E* **83(6)**:066316 DOI 10.1103/physreve.83.066316.

Schnabel V, Struijk JJ. 1999. Magnetic and electrical stimulation of undulating nerve fibres: a simulation study. *Medical & Biological Engineering & Computing* **37(6)**:704–709 DOI 10.1007/bf02513371.

Schnabel V, Struijk JJ. 2001. Evaluation of the cable model for electrical stimulation of unmyelinated nerve fibers. *IEEE Transactions on Biomedical Engineering* **48(9)**:1027–1033 DOI 10.1109/10.942593.

Schwan HP. 1957. Electrical properties of tissue and cell suspensions. *Advances in Biological and Medical Physics* **5**:147–209 DOI 10.1016/b978-1-4832-3111-2.50008-0.

Selimbeyoglu A, Parvizi J. 2010. Electrical stimulation of the human brain: perceptual and behavioral phenomena reported in the old and new literature. *Frontiers in Human Neuroscience* **4**:46 DOI 10.3389/fnhum.2010.00046.

Sotiropoulos SN, Steinmetz PN. 2007. Assessing the direct effects of deep brain stimulation using embedded axon models. *Journal of Neural Engineering* **4(2)**:107–119 DOI 10.1088/1741-2560/4/2/011.

Stratton J. 1941. *Electromagnetic theory*. New York: McGraw-Hill.

Struijk JJ, Durand DM. 1998. Magnetic peripheral nerve stimulation: axial verses transverse fields. In: *Proceedings BMES/EMBS, Atlanta*, 469.

Struijk JJ, Schnabel V. 2001. Difference between electrical and magnetic nerve stimulation: a case for transverse field. *Proceedings of the 23rd Annual International Conference of IEEE*, Piscataway: IEEE, 885–887.

Sturrock RR. 1980. Myelination of the mouse corpus callosum. *Neuropathology and Applied Neurobiology* **6(6)**:415–420 DOI 10.1111/j.1365-2990.1980.tb00219.x.

Susil R, Semrov D, Miklavcic D. 1998. Electric field-induced transmembrane potential depends on cell density and organization. *Electro- and Magnetobiology* **17(3)**:391–399 DOI 10.3109/15368379809030739.

Teruel MN, Meyer T. 1997. Electroporation-induced formation of individual calcium entry sites in the cell body and processes of adherent cells. *Biophys J* **73**:1785–1796 DOI 10.1016/S0006-3495(97)78209-2.

Tyler WJ. 2012. The mechanobiology of brain function. *Nature Reviews Neuroscience* **13(12)**:867–878 DOI 10.1038/nrn3383.

Wang B, Aberra AS, Grill WM, Peterchev AV. 2018. Modified cable equation incorporating transverse polarization of neuronal membranes for accurate coupling of electric fields. *Journal of Neural Engineering* **15(2)**:026003 DOI 10.1088/1741-2552/aa8b7c.

Wang B, Grill WM, Peterchev AV. 2018. Coupling magnetically induced electric fields to neurons: longitudinal and transverse activation. *Biophysical Journal* **115**:95–107 DOI 10.1016/j.bpj.2018.06.004.

Waxman SG, Black JA, Stys PK, Ransom BR. 1992. Ultrastructural concomitants of anoxic injury and early post-anoxic recovery in rat optic nerve. *Brain Research* **574(1–2)**:105–119 DOI 10.1016/0006-8993(92)90806-k.

While PT, Forbes LK. 2004. Electromagnetic fields in the human body due to switched transverse gradient coils in MRI. *Physics in Medicine and Biology* **49(13)**:2779–2798 DOI 10.1088/0031-9155/49/13/002.

Ye H, Buttigieg J, Wan Y, Wang J, Figley S, Fehlings MG. 2012. Expression and functional role of BK channels in chronically injured spinal cord white matter. *Neurobiology of Disease* **47(2)**:225–236 DOI 10.1016/j.nbd.2012.04.006.

Ye H, Cotic M, Carlen PL. 2007. Transmembrane potential induced in a spherical cell model under low-frequency magnetic stimulation. *Journal of Neural Engineering* **4(3)**:283–293 DOI 10.1088/1741-2560/4/3/014.

Ye H, Cotic M, Fehlings MG, Carlen PL. 2011. Transmembrane potential generated by a magnetically induced transverse electric field in a cylindrical axonal model. *Medical & Biological Engineering & Computing* **49(1)**:107–119 DOI 10.1007/s11517-010-0704-0.

Ye H, Cotic M, Kang EE, Fehlings MG, Carlen PL. 2010. Transmembrane potential induced on an internal organelle by a time-varying magnetic field: a model study. *Journal of NeuroEngineering and Rehabilitation* **7(1)**:12 DOI 10.1186/1743-0003-7-12.

Ye H, Curcuru A. 2016. Biomechanics of cell membrane under low-frequency time-varying magnetic field: a shell model. *Medical & Biological Engineering & Computing* **54(12)**:1871–1881 DOI 10.1007/s11517-016-1478-9.

Ye H, Steiger A. 2015. Neuron matters: electric activation of neuronal tissue is dependent on the interaction between the neuron and the electric field. *Journal of NeuroEngineering and Rehabilitation* **12(1)**:65 DOI 10.1186/s12984-015-0061-1.

Yu H, Zheng C, Wang Y. 2005. A new model and improved cable function for representing the activating peripheral nerves by a transverse electric field during magnetic stimulation. *Proceedings of the 2nd International IEEE EMBS Conference on Neural Engineering.* Piscataway: IEEE.

Zhao H, Steiger A, Nohner M, Ye H. 2015. Specific intensity direct current (DC) electric field improves neural stem cell migration and enhances differentiation towards *β*III-Tubulin+ Neurons. *PLOS ONE* **10(6)**:e0129625 DOI 10.1371/journal.pone.0129625.